COVER PAGE

Bibliographical reference

Application of Dirichlet-to-Neumann Map to Calculation of Band Gaps for Scalar Waves in Two-Dimensional Phononic Crystals, Feng-Lian Li and Yue-Sheng Wang, Acta Acustica **vol. 97** (Number 2), 2011, pp. 284-290

DOI

https://doi.org/10.3813/AAA.918408

Acta Acustica united with Acustica
Vol. 97 (2011) 284 – 290

DOI 10.3813/AAA.918408

Application of Dirichlet-to-Neumann Map to Calculation of Band Gaps for Scalar Waves in Two-Dimensional Phononic Crystals

Feng-Lian Li, Yue-Sheng Wang
Institute of Engineering Mechanics, Beijing Jiaotong University, Beijing 100044, China. yswang@bjtu.edu.cn

Summary
This paper is aimed at applying Dirichlet-to-Neumann (DtN) map to calculate the band gaps of scalar waves in a two-dimensional phononic crystal which is composed of circular cylinders embedded in a host medium in either square or triangular lattice. Detailed computation is performed for both solid/solid and fluid/fluid systems with emphasis on comparison to the plane wave expansion method. The numerical results show some merits of the DtN method. Its computing cost to obtain the results of high accuracy is very low, especially for higher frequency computation or for systems with large acoustic mismatch. Another feature of the DtN method is that it can yield band structures at an arbitrary frequency interval which does not necessarily start from zero.
PACS no. 43.20.Fn

1. Introduction

The study of propagation of waves in inhomogeneous media is a problem of wide interest. The last decades have witnessed great research interest, both experimentally and theoretically, in phononic crystals [1] which are artificial two- or three-dimensional periodic elastic/acoustic composites. The emphasis was laid on the existence of complete band gaps within which sound, vibrations and phonons are strongly attenuated. This is of interest for applications such as noise control, design of new transducers and filters, etc.

One fundamental problem for design and optimization of phononic crystals and related devices is to compute the band structures (dispersion curves) of phononic crystals. Several methods have been developed, which include the plane-wave expansion method (PWE) [1, 2, 3], the transfer matrix (TM) method [4], the multiple scattering theory (MST) method [5, 6], the finite element method (FEM) [7, 8, 9], the wavelet method [10, 11], the lumped-mass (LM) method [12], the boundary element method (BEM) [13], etc. The FEM and LM methods discretize the unit cell; while the PWE and wavelet methods utilize the eigenfunction expansions. They yield linear eigenvalue equations with the frequency as the eigenvalues for given Bloch wave vectors. The eigenvalue equations, although generally with the large matrix size, can yield the stable results for a desired frequency region starting from zero. In the BEM and MST methods the linear eigenvalue equations are replaced by nonlinear ones. Although the nonlinear approach gives rise to much smaller matrices, the eigenvalues must be searched one-by-one from the condition that a matrix becomes singular. The finite difference time domain (FDTD) method [14, 15] has also been developed for bandgap calculation, but it cannot yield the band structures directly and is time consuming for systems with large acoustic mismatch.

Recently, Yuan and Lu [16, 17] developed a method based on the Dirichlet-to-Neumann (DtN) map to compute the band structures of two-dimensional photonic crystals with circular cylindrical scatterers. The DtN map, which is an operator that maps the wave field on the boundary of a unit cell to its normal derivative there, is widely used in solving acoustic problems of the scattering or waveguide [18, 18, 19, 20, 21]. Yuan and Lu's method mainly relies on the construction of the DtN map. The computation of the map uses a cylindrical wave expansion. This gives rise to accurate approximations of the DtN map with relatively small matrices [16, 17]. A linear eigenvalue problem, where the eigenvalue is related to the Bloch wave vector, is obtained. Compared with the other methods, the DtN method costs much lower computing time and can yield band structures in an arbitrary frequency region which is not necessarily from zero. In this paper, we will extend the method to calculate the band gaps of scalar waves in a two-dimensional phononic crystal.

The outline of this paper is as follows. In section 2, the basic scalar wave equations and the boundary conditions in a unit cell are introduced. A matrix approximation to the DtN map is constructed by using the cylindrical wave expansions, and the linear eigenvalue problems are formulated in section 3 for both square and triangular lattices. Then we give some numerical examples to show the efficiency of the method in section 4, followed by conclusions in section 5.

Received 20 January 2010,
accepted 3 January 2011.

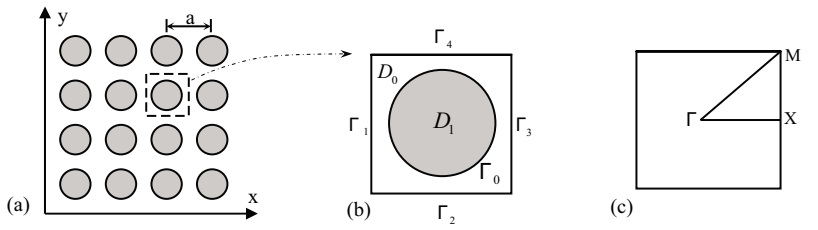

Figure 1. The structure of the square lattice with circular cylindrical inclusions (a), its unit cell (b) and the corresponding first Brillouin zone (c).

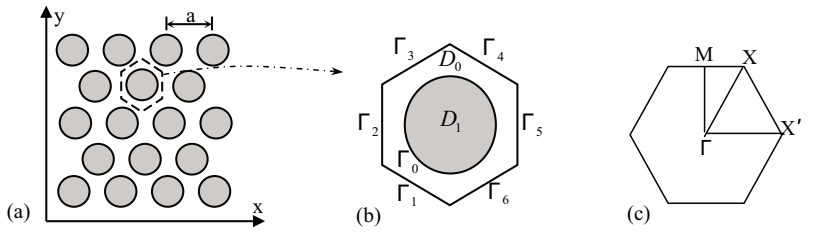

Figure 2. The structure of the triangle lattice with circular cylindrical inclusions (a), its unit cell (b) and the corresponding first Brillouin zone (c).

2. Basic equations and boundary conditions

A two-dimensional (2D) phononic crystal is composed of circular cylinders of radius r_c forming a square (Figure 1a) or triangle (Figure 2a) array with the lattice constant a in an isotropic elastic matrix. There is translational invariance in the direction parallel to the cylinders (z-axis) and the system has two-dimensional periodicity in the transverse plane(x-y plane). Both solid–solid system and fluid–fluid system will be considered in this paper. It is known that only longitudinal waves propagate in fluid media. However, elastic waves in solids are generally mixed longitudinal and transverse modes propagating with different velocities. If the propagation of the elastic waves is limited to the transverse plane normal to the cylinder axis, an independent purely transverse mode may propagate in the system. Both longitudinal mode in fluids and purely transverse mode in solids are scalar modes of which the governing equations are similar to those of the two-dimensional electromagnetic waves even though they have different physical meanings and boundary conditions [16, 17]. In the present paper, to illustrate the ideas involved we will consider these simple situations.

We first consider the purely transverse wave with the only non-zero displacement component $u_z(\boldsymbol{r})$ along z-axis. The governing Helmholtz equation is

$$\mu_j \nabla^2 u_{zj}(\boldsymbol{r}) + \rho_j \omega^2 u_{zj}(\boldsymbol{r}) = 0, \quad \boldsymbol{r} \in D_j, \quad j = 0, 1, \qquad (1)$$

where $\boldsymbol{r} = (x, y)$ is the position vector; $\nabla = (\partial/\partial x, \partial/\partial y)$ is the vector Laplacian; ω is the angular frequency; ρ_j and μ_j are the mass density and shear modulus with the subscript $j = 0$ and 1 representing the matrix (D_0) and inclusion (D_1), see Figures 1 and 2.

Due to the periodicity of the system, we can restrict our attention to a unit cell (Figures 1b and 2b). At the interface Γ_0 between the matrix and the inclusion, the displacement and traction are continuous, which states

$$u_{zl}(\boldsymbol{r}) = u_{z0}(\boldsymbol{r}), \quad \mu_1 \frac{\partial u_{zl}(\boldsymbol{r})}{\partial \boldsymbol{n}} = \mu_0 \frac{\partial u_{z0}(\boldsymbol{r})}{\partial \boldsymbol{n}} \quad \boldsymbol{r} \in \Gamma_0, \qquad (2)$$

where $\boldsymbol{n}$ is the normal vector of Γ_0. The first part of the above equation is related to the Dirichlet boundary condition and the second one is related to the Neumman boundary condition, respectively.

Acoustic waves propagating in ideal fluid media are also scalar wave modes. Let us consider a periodic composite medium composed of fluid inclusions embedded in a dissimilar fluid [22]. If we introduce a scalar potential function $\varphi(x, y)$ defined by $\rho \boldsymbol{u} = \nabla \varphi(x, y)$ where $\boldsymbol{u}$ is the displacement vector, then acoustic wave equations in the matrix and inclusions may be written as

$$\rho_j^{-1} \nabla^2 \varphi_j(\boldsymbol{r}) + \lambda_j^{-1} \omega^2 \varphi_j(\boldsymbol{r}) = 0, \quad \boldsymbol{r} \in D_j, \quad j = 0, 1, \qquad (3)$$

where λ_j is the elastic modulus of the fluids. In this case, the potential and normal displacement at the interface between the matrix and inclusion are continuous, that is

$$\varphi_1(\boldsymbol{r}) = \varphi_0(\boldsymbol{r}), \quad \frac{1}{\rho_1} \frac{\partial \varphi_1(\boldsymbol{r})}{\partial \boldsymbol{n}} = \frac{1}{\rho_0} \frac{\partial \varphi_0(\boldsymbol{r})}{\partial \boldsymbol{n}} \quad \boldsymbol{r} \in \Gamma_0. \qquad (4)$$

It is noted that eqations (3) and (4), when ρ_j^{-1} and λ_j^{-1} are replaced by μ_j and ρ_j respectively, are identical to equations (1) and (2). Therefore the following derivation will be presented based on equations (1) and (2).

3. Construction of the Dirichlet-to-Neumann map and eigenvalue equations

The Dirichlet-to-Neumann map is a map operator Λ that maps the displacement $\boldsymbol{u}$ on the boundary of the unit cell to its normal derivative, i.e.

$$\Lambda \boldsymbol{u}\big|_{\Gamma_k} = \frac{\partial u}{\partial \boldsymbol{n}}\bigg|_{\Gamma_k}, \qquad (5)$$

where Γ_k is the boundary of the unit cell (with $k = 1, \ldots, 4$ for the square lattice and $k = 1, \ldots, 6$ for the triangular lattice) and $\boldsymbol{n}$ is their corresponding normal vector. Hereafter, the subscripts of u will be omitted without confusing. Next we will give a brief introduction to construct the matrix approximation to Λ. For the detailed process, we refer to [16, 17].

According to the cylindrical wave expansion [23], we can write the general solution of the wave equation (1) using the polar coordinate system (r, θ) as

$$u(x, y) = \sum_{m=-\infty}^{\infty} C_m \Phi_m(r, \theta), \quad \Phi_m(r, \theta) = \phi_m(\boldsymbol{r}) \mathrm{e}^{\mathrm{i}m\theta}, \quad (6)$$

where

$$\phi_m(\boldsymbol{r}) = \begin{cases} A_m J_m(k_1 r), & r < r_c, \\ B_m J_m(k_0 r) + Y_m(k_0 r), & r > r_c. \end{cases} \quad (7)$$

In the above equation, $J_m(..)$ and $Y_m(..)$ are the first and second kinds of Bessel functions of the mth order; $k_j = \omega / c_j$ are the wave numbers of the matrix ($j = 0$) and inclusion ($j = 1$) where c_j represents the transverse wave velocity in the solids or the acoustic wave velocity in the fluids. The coefficients A_m and B_m can be solved from the interface conditions equation (2).

In the discrete case for the square lattice, we select N points on each edge of the square unit cell; and simultaneously truncate equation (6) from $m = -2N$ to $2N-1$. This gives rise to a $4N \times 4N$ matrix Λ_1 that maps the coefficients $\{C_m\}$ to the values of $\boldsymbol{u}$ at these points. Its elements are $(\Lambda_1)_{l,m} = \Phi_m(r_l, \theta_l)$ where the subscript $l = 0 \sim 4N$ representing the lth numbered point on the unit cell edges. Similarly, if we evaluate the normal derivative of $\boldsymbol{u}$ at the same points, we obtain a $4N \times 4N$ matrix Λ_2 that maps $\{C_m\}$ to the normal derivatives at these points. Its elements are given by $(\Lambda_2)_{l,m} = \partial \Phi_m(r_l, \theta_l) / \partial \boldsymbol{n}(l)$. Finally from equation (5), we obtain the following matrix approximation of the DtN map

$$\Lambda = \Lambda_2 \Lambda_1^{-1}. \quad (8)$$

Now the Dirichlet-to-Neumann map is approximated by a $4N \times 4N$ matrix for the square.

To analyze the band structures, we consider the following Bloch mode solutions [24] of equation (1),

$$\boldsymbol{u}(x, y) = \mathrm{e}^{\mathrm{i}(k_x x + k_y y)} \phi(x, y), \quad (9)$$

where (k_x, k_y) is the real Bloch wave vector and $\phi(x, y)$ follows the same periodic condition as the lattice.

Application of the Bloch theorem (equation 9) to the boundary of the square lattice leads to

$$\begin{aligned} \boldsymbol{u}\big|_{\Gamma_3} &= \alpha \boldsymbol{u}\big|_{\Gamma_1}, \quad \boldsymbol{u}\big|_{\Gamma_4} = \beta \boldsymbol{u}\big|_{\Gamma_2}, \\ \frac{\partial \boldsymbol{u}}{\partial y}\Big|_{\Gamma_3} &= \alpha \frac{\partial \boldsymbol{u}}{\partial y}\Big|_{\Gamma_1}, \quad \frac{\partial \boldsymbol{u}}{\partial x}\Big|_{\Gamma_4} = \alpha \frac{\partial \boldsymbol{u}}{\partial x}\Big|_{\Gamma_2}, \end{aligned} \quad (10)$$

where $\alpha = \mathrm{e}^{\mathrm{i}k_x a/2}$ and $\beta = \mathrm{e}^{\mathrm{i}k_y a/2}$. The above relations finally can yield nonlinear eigenvalue equations of which the solution is not a nontrivial task. Fortunately, if we are interested in the band gap, only the dispersion curves along the boundary, of the irreducible Brillouin zone (i.e., $\Gamma - X - M - \Gamma$, see Figure 1c) are necessary. In this case, the nonlinear eigenvalue equations reduce to linear ones. For the square lattice, the finally obtained linear eigenvalue equation may be written as [16]

$$\eta \begin{bmatrix} \mathcal{A} & 0 \\ 0 & I \end{bmatrix} \begin{bmatrix} V \\ U \end{bmatrix} + \begin{bmatrix} \mathcal{B} & \mathrm{C} \\ -I & 0 \end{bmatrix} \begin{bmatrix} V \\ U \end{bmatrix} = 0. \quad (11)$$

where I is the identity matrix and $V = \eta U = \eta (u_{\Gamma_1}, u_{\Gamma_2})^T$ with the superscript "T" representing the transposition. The detailed expressions of the $2N \times 2N$ matrices $\mathcal{A}$, $\mathcal{B}$ and C can be found in [16].

The eigenvalue η to be determined from equation (11) is related to the Bloch wave vector, (k_x, k_y), by $\eta = \mathrm{e}^{\mathrm{i}k_x a}$ or $\eta = \mathrm{e}^{\mathrm{i}k_y a}$. Since the materials considered here are elastic and non-dissipative media, the values of k_x and k_y are real. Therefore only the eigenvalues which satisfy $|\eta| = 1$ are the values that we need and can be saved for each frequency. In calculation, we replace $|\eta| = 1$ by $||\eta| - 1| \le \varepsilon$ where the small positive number ε is generally taken to be $10^{-6} \sim 10^{-8}$.

For the triangle lattice, we choose N points on each edge of the hexagonal unit cell; and truncate equation (6) from $m = -3N$ to $3N - 1$. By the similar process, the Dirichlet-to-Neumann map is approximated by a $6N \times 6N$ matrix. Application of the Bloch theorem to the boundary of the triangular lattice leads to

$$\begin{aligned} \boldsymbol{u}\big|_{\Gamma_4} &= \alpha\beta \boldsymbol{u}\big|_{\Gamma_1}, \quad \boldsymbol{u}\big|_{\Gamma_5} = \alpha \boldsymbol{u}\big|_{\Gamma_2}, \\ \beta \boldsymbol{u}\big|_{\Gamma_6} &= \alpha \boldsymbol{u}\big|_{\Gamma_3}, \quad \frac{\partial \boldsymbol{u}}{\partial \boldsymbol{n}}\Big|_{\Gamma_4} = \alpha\beta \frac{\partial \boldsymbol{u}}{\partial \boldsymbol{n}}\Big|_{\Gamma_1}, \\ \frac{\partial \boldsymbol{u}}{\partial \boldsymbol{n}}\Big|_{\Gamma_5} &= \alpha \frac{\partial \boldsymbol{u}}{\partial \boldsymbol{n}}\Big|_{\Gamma_2}, \quad \beta \frac{\partial \boldsymbol{u}}{\partial \boldsymbol{n}}\Big|_{\Gamma_6} = \alpha \frac{\partial \boldsymbol{u}}{\partial \boldsymbol{n}}\Big|_{\Gamma_3}, \end{aligned} \quad (12)$$

where $\alpha = \mathrm{e}^{\mathrm{i}k_x a/2}$ and $\beta = \mathrm{e}^{\mathrm{i}k_y \sqrt{3} a/2}$. Only the dispersion curves along the boundary of the irreducible Brillouin zone (i.e., $\Gamma - X - M - \Gamma$, see Figure 2c) are necessary. Finally, we can get a linear eigenvalue equation that is

$$\eta \begin{bmatrix} \mathcal{M}_4 & 0 & 0 & 0 \\ 0 & I & 0 & 0 \\ 0 & 0 & I & 0 \\ 0 & 0 & 0 & I \end{bmatrix} V + \begin{bmatrix} \mathcal{M}_3 & \mathcal{M}_2 & \mathcal{M}_1 & \mathcal{M}_0 \\ -I & 0 & 0 & 0 \\ 0 & -I & 0 & 0 \\ 0 & 0 & -I & 0 \end{bmatrix} V = 0, \quad (13)$$

where

$$V = \left[\eta^3 U^T, \eta^2 U^T, \eta U^T, U^T\right]^T$$

and

$$U = \left(u_{\Gamma_1}, u_{\Gamma_2}, u_{\Gamma_3}\right)^T.$$

The detailed expressions of the $3N \times 3N$ matrices $\mathcal{M}_0 \sim \mathcal{M}_4$ are given in [17]. Equation (13) is a linear eigenvalue problem of $12N \times 12N$ matrix. It can be determined in the same way as the square lattice.

It is particularly noticed that, unlike other methods such as PWE, Wavelet and FEM etc., equations (11) and (13) yield the Bloch wave vector $\boldsymbol{k}$ with the frequency being given. This enables us to calculate the band structures in a particular frequency region which does not necessarily start from zero.

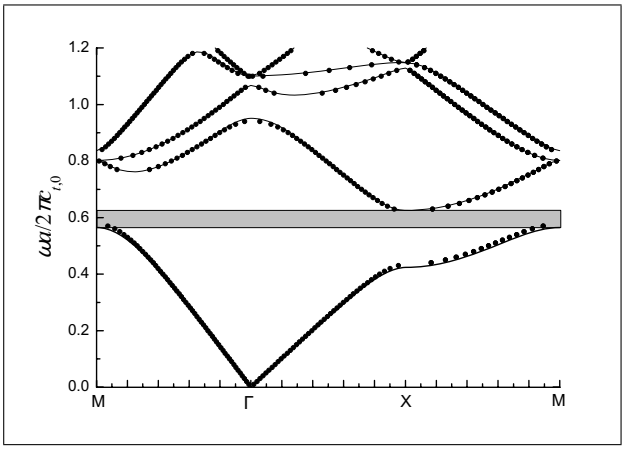

Figure 3. Band structures of the transverse modes in a 2D square lattice consisting of Al cylinders in the Ni matrix with filling fraction $f = 0.75$. The scattered dots and solid lines are from the calculations of the DtN method and the PWE method (with 441 plane waves), respectively. The shadowed region defines the complete band gaps.

4. Numerical results and discussion

In this section, numerical examples are presented for different systems including solid/solid and fluid/fluid lattices in square and triangle. We particularly discuss the accuracy and efficiency of the present method by comparing the results with those obtained by the PWE method.

4.1. Al/Ni lattice

As the first example to test the method, we consider the system studied in one of the earliest papers on phononic crystals by Kushwaha *et al.* [1], i.e. purely transverse waves propagating in a square lattice of alumina (Al) cylinders embedded in the nickel (Ni) matrix. The material parameters including the density and the transverse velocity are: $\rho_0 = 8.936 \cdot 10^3$ kg/m^3 and $c_0 = 7.925$ km/s for Ni; and $\rho_1 = 2.697 \cdot 10^3$ kg/m^3 and $c_1 = 3.110$ km/s for Al. The impedance ($\rho_j c_j$) ratio of the Ni and Al is 8.4. The filling fraction is $f = \pi r_c^2/a^2 = 0.75$, where r_c is the radius of Al cylinders and a is the lattice constant. Figure 3 illustrates the band structures calculated by the DtN method (scattered dots) and the PWE method (solid lines). The vertical axis is the normalized frequency $\omega a/2\pi c_0$. The horizontal axis represents the edges of the irreducible Brillouin zone. In the DtN method, the numerical tests show that $N = 6 \sim 10$ can yield convergent results. Here we choose $N = 8$, which implies that the DtN map is constructed from a cylindrical wave expansion of 32 terms and the linear eigenvalue problem involves 32×32 matrices. In the PWE method, 441 plane waves are involved [9]. From Figure 3 we observe that the results from the two methods are almost identical except a slight difference when the wave vector tends to the point M.

4.2. Au/Epoxy lattice

The above calculated phononic crystal has small acoustic mismatch. In this case the PWE method can give convergent results with fewer plane waves. To check the efficiency of the DtN method, we next consider purely transverse waves propagating in square lattice and triangular lattices of aurum (Au) cylinders embedded in the epoxy matrix. The material parameters are: $\rho_0 = 1.18 \cdot 10^3$ kg/m^3 and $c_0 = 1.157$ km/s for epoxy; and $\rho_1 = 1.95 \cdot 10^4$ kg/m^3 and $c_1 = 1.239$ km/s for Au. The impedance ($\rho_j c_j$) ratio of the Au and epoxy is 17.7. The filling fraction is $f = 0.4$. Here we also chose $N = 8$ on each edge of the unit cell. The band structures for the square and triangular lattice are plotted in Figures 4a and 4b, respectively, with comparison to the PWE method (where 441 plane waves are used). From the figures we can observe two complete band gaps in the shown frequency intervals. The first band gap is larger than the second one and the width of the first band gap in the square lattice is smaller than that in the triangular lattice. Whether in the square lattice or in the triangular lattice, the first band gaps computed by the two methods are almost identical; but the second band gap has a little difference. This, we believe, is due to the poor convergence of the PWE method in higher frequencies. To demonstrate this fact, we use more plane waves, for example, 961 plane waves, in the PWE method and list the band-gap regions computed by the DtN and PWE(with

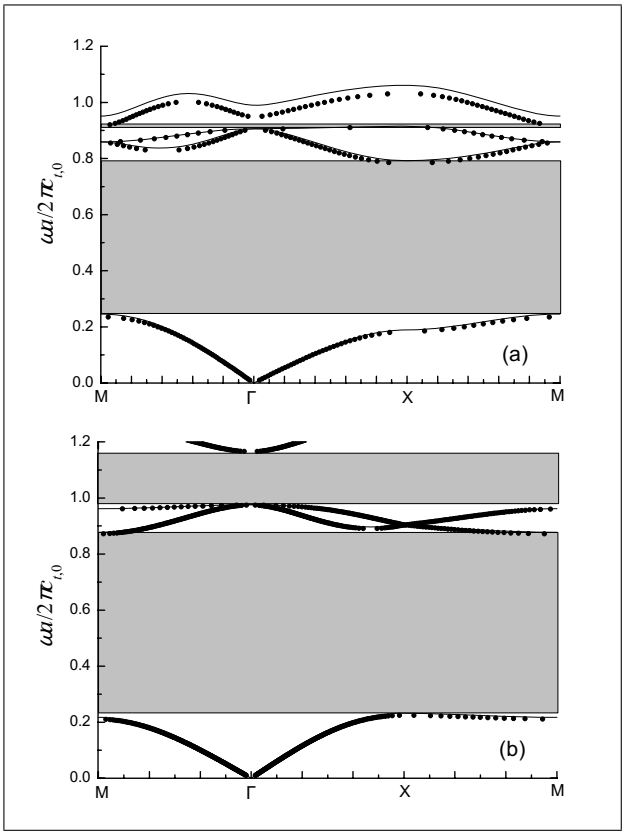

Figure 4. Band structures of the transverse modes in 2D phononic crystals consisting of Au cylinders in the epoxy matrix with filling fraction $f = 0.4$, (a) the square lattice, and (b) the triangular lattice. The scattered dots and solid lines are from the calculations of the DtN method and the PWE method (with 441 plane waves), respectively. The shadowed regions define the complete band gaps.

Table I. Comparison of the bandgaps computed by two methods for the Au/epoxy system. No.: Bandgap number

	No.	PWE (441)	PWE (961)	DtN
□	1	[0.245,0.792]	[0.240,0.789]	[0.235,0.785]
	2	[0.906,0.951]	[0.906,0.942]	[0.905,0.939]
△	1	[0.231,0.877]	[0.229,0.875]	[0.224,0.872]
	2	[0.976,1.230]	[0.975,1.201]	[0.974,1.187]

Table III. Computing time of the two methods for the Au/epoxy system (CPU time is in seconds).

	PWE (441)	PWE (961)	DtN
□	270.84	2962.50	5.22
△	284.25	3017.37	25.43

441 and 961 plane waves) methods in Table I. We can find the results from the PWE method with more (961) plane waves are nearly identical to those of the DtN method. This is similar to the results of the photonic crystals in [16, 17]. The poor convergence and precision of the PWE method for the phononic crystals with large acoustic mismatch [14] are due to the Gibbs effect [25, 26]. The present DtN method however shows good convergence, see Table II which gives the calculated results with increasing value of N.

We also compare the computing time of the two methods to obtain the whole band structures shown in Figures 4a and 4b, see Table III. To illustrate Figures 4a and 4b, we have calculated 240 frequencies using the DtN method and 60 Bloch wave vectors using the PWE method. It is shown that the computing cost of the present method is very low.

4.3. Water/Mercury lattice

Finally we consider acoustic waves in fluid/fluid phononic crystals. The systems are composed of a square or triangular lattice of water cylinders surrounded by the mercury medium. The material parameters are: $\rho_1 = 1.025 \cdot 10^3\,\mathrm{kg/m^3}$, $c_1 = 1531\,\mathrm{m/s}$ for water; and $\rho_0 = 13.6 \cdot 10^3\,\mathrm{kg/m^3}$, $c_0 = 1450\,\mathrm{m/s}$ for mercury at 25 °C. The impedance ($\rho_j c_j$) ratio of the mercury and water is 12.6. The filling fraction is $f = 0.35$. In calculation, we choose on each edge of the unit cell and then obtain a linear eigenvalue problem involving 24 × 24 or 72 × 72 matrices. Figures 5a and 5b illustrate the band structures for the square and triangular lattices respectively, which are obtained by the present method and the PWE method with 441 plane waves. From the figure we can see that the results obtained by the PWE method lie slightly above those obtained by the DtN method especially in higher frequencies. This trend is more obvious for the triangular lattice. This is because large acoustic mismatch between water and mercury makes the convergence of the PWE calculation very slow. We have re-computed the results using the PWE method by taking 961 and 1681 plane waves. The obtained band-gap regions are listed in Table IV. It is

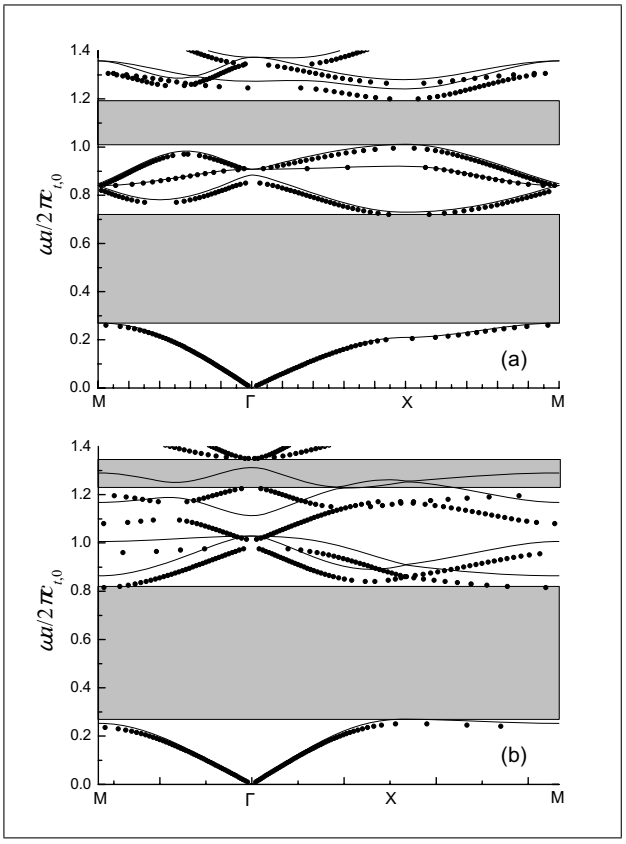

Figure 5. Band structures of 2D phononic crystals with water cylinders surrounded by mercury host, (a) the square lattice, and (b) the triangular lattice. The filling fraction is $f = 0.35$. The scattered dots and solid lines represent the results calculated by the DtN method and the PW method (with 441 plane waves), respectively. The shadowed regions define the complete band gaps.

seen that, with the increase of the number of plane waves used in the PWE method, the results converge to those of the DtN method. However more plane waves used implies much more computing cost, see Table V where the computing time of the two methods to obtain the whole band structures are listed (we have calculated 280 frequencies using the DtN method and 60 Bloch wave vectors using the PWE method). It is shown that the computing time of the present DtN method to obtain the results of high accuracy is extremely less.

5. Conclusions

In this paper, we have applied the Dirichlet-to-Neumann method from solving the short range wave propagation problems (photonic crystals) to compute the band structures of the long range acoustic waves propagating in phononic crystals. Two-dimensional solid/solid and fluid/fluid systems with either square or triangular lattice are considered in the numerical examples. The results show its some merits in comparison with the PWE method, especially, in the case of large acoustic mismatch. It gives rise to a linear eigenvalue problem with relatively small matrices in comparison with other methods such as PWE,

Table II. Convergence of the method for Au/epoxy systems (the dimensionless frequency is 0.1). $N = 2\pi k/a$ (ΓX).

lattice	4	5	6	7	8	9	10
square	0.1934 2885	0.192 25545	0.192 23341	0.192 28374	0.192 21331	0.192 21332	0.192 21331
triangular	0.190 40941	0.190 31852	0.190 31561	0.190 31968	0.190 31964	0.190 31949	0.190 31950

Table IV. Comparison of the bandgaps computed by two methods for the water/mercury system.

	No.	PWE (441)	PWE (961)	PWE (1681)	DtN method
square	1	[0.269,0.729]	[0.266,0.725]	[0.264,0.723]	[0.264,0.723]
	2	[1.011,1.241]	[1.006,1.223]	[1.004,1.217]	[0.998,1.210]
triangular	1	[0.269,0.863]	[0.267,0.860]	[0.266,0.859]	[0.262,0.832]
	2	[1.311,1.435]	[1.303,1.428]	[1.238,1.425]	[1.225,1.358]

Table V. Computing time of the two methods for the water/mercury system (CPU time is in seconds).

	PWE (441)	PWE (961)	PWE (1681)	DtN
□	278.79	30198.30	162651.16	6.97
△	293.27	3111.69	16873.57	22.31

Wavelet, FEM, etc., and thus has less computational cost and is memory-saving as well as time-saving. It can yield accurate results with fast convergence and negligible increasing of computing effort for systems with large acoustic mismatch. These advantages make it possible for easy calculations at higher frequencies where the PWE method encounters difficulties. Another important feature of the DtN method is that it can yield band structures at an arbitrary frequency interval which does not necessarily start from zero. We know that the developed method does have some limitations. For instance, the method is only valid for circular cylindrical scatterers because the explicit DtT map can be obtained only in this situation; and it fails for anisotropic materials because the cylindrical wave expansions (equation 7) for the displacement does not hold in this case.

Although we only study the scalar waves in 2D phononic crystals in the present paper, the developed method is expected to be extended to the mixed wave modes, which is now under our consideration. The method may treat the case of irregular shaped inclusions when combined with the boundary integral equation method [27] or calculate the transmission properties of phononic crystals [28].

Acknowledgement

The authors thank the National Natural Science Foundation of China (Grant No.10632020) for the financial support.

References

[1] M. S. Kushwaha, P. Halevi: Acoustic band structure of periodic elastic composites. Phys. Rev. Lett. **71** (1993) 2022–2025.

[2] M. M. Sigalas, E. N. Economou: Elastic and acoustic wave band structure. J. Sound. Vib. **158** (1992) 377–382.

[3] T. T. Wu, Z. G. Huang, S. Lin: Surface and bulk acoustic waves in two-dimensional phononic crystal consisting of materials with general anisotropy. Phys. Rev. B **69** (2004) 094301.

[4] R. E. Camley, B. Djafari-Rouhani, L. Dobrzynski: Transverse elastic waves in periodically layered infinite and semi-infinite media. Phys. Rev. B **27** (1983) 7318–7329.

[5] M. Kafesaki, E. N. Economou: Multiple-scattering theory for three-dimensional periodic acoustic composites. Phys. Rev. B **60** (1999) 11993–12001.

[6] J. Mei, C. Qiu, Z. Liu: Multiple-scattering theory for out-of-plane propagation of elastic waves in two-dimensional phononic crystals. J. Phys-condens. Mater **17** (2005) 3735–3757.

[7] W. Axmann, P. Kuchment: An efficient finite element method for computing spectra of photonic and acoustic band-gap materials. I. Scalar case. J. Comput. Phys **150** (1999) 468–481.

[8] J. B. Li, Y. S. Wang, C. Zhang: Finite element method for analysis of band structures of phononic crystals. Proc. 2008 IEEE Inter. Ultrasonics Symp 1-4, 2008, 1468–1471.

[9] I. Harari, M. Slavutin, E. Turkel: Analytical and numerical studies of a finite element PML for the Helmholtz equation. J. Comput. Acoustics (2000) 8121–8137.

[10] Z. Z. Yan, Y. S. Wang: Wavelet-based method for computing elastic band gaps of one-dimensional phononic crystals. Sci. China - Phys. Mech. Astron **50** (2007) 622–630.

[11] Z. Z. Yan, Y. S. Wang: Wavelet-based method for calculating elastic band gaps of two-dimensional phononic crystals. Phys. Rev. B **74** (2006) 224303.

[12] G. Wang, J. H. Wen, Y. Z. Liu: Lumped-mass method for the study of band structure in two-dimensional phononic crystals. Phys. Rev. B **69** (2004) 184302.

[13] F. L. Li, Y. S. Wang: Band gap analysis of two-dimensional phononic crystals based on boundary element method. Proc. 2008 IEEE Inter. Ultrasonics Symp 1-4, 2008, 245–248.

[14] Y. Tanaka, Y. Tomoyasu: Band structure of acoustic waves in phononic lattices: Two-dimensional composites with

large acoustic mismatch. Phys. Rev. B **62** (2000) 7387–7392.

[15] G. Wang, J. H. Wen, X. Y. Han: Finite difference time domain method for the study of band gap in two-dimensional phononic crystals. Chinese. Phys. Lett. **52** (2003) 1943–1947.

[16] J. H. Yuan, Y. Y. Lu: Photonic bandgap calculations with Dirichlet-to-Neumann maps. J. Opt. Soc. Am. A **23** (2006) 3217–3222.

[17] J. H. Yuan, Y. Y. Lu: Computing photonic band structures by Dirichlet-to-Neumann maps: The triangular lattice. Opt. Commu. **273** (2007) 114–120.

[18] M. Malhotra, P. M. Pinsky: Efficient computation of multi-frequency far-field solutions of the Helmholtz equation using Padé approximation. J. Comput. Acoustics **8** (2000) 223–240.

[19] J. Zhu, Y. Y. Lu: Validity of one-way models in the weak range dependence limit. J. Comput. Acoustics **12** (2004) 55–66.

[20] D. A. Mitsoudis: Near-and far-field boundary conditions for a finite element method for the Helmholtz equation in in axisymmetric problems of underwater acoustics. Acta Acustica united with Acustica **93** (2007) 888–898.

[21] W. F. Pan, Y. X. You, G. P. Miao, Z. Q. Li: A coupled FE and DtN mapping method for the exterior problem of the Helmholtz equation in an oceanic waveguide. Acta Acustica united with Acustica **94** (2008) 301–309.

[22] M. S. Kushwaha, P. Halevi: Giant acoustic stop bands in two-dimensional periodic arrays of liquid cylinders. Appl. Phys. Lett. **69** (1996) 31–33.

[23] Y. H. Pao, C. C. Mao: Diffraction of elastic waves and dynamic stress concentration. Adam Hilger, 1973.

[24] N. W. Ashcroft, N. D. Mermin: Solid state physics. World Publication, 2004.

[25] L. F. Li: Use of Fourier series in the analysis of discontinuous periodic structures. J. Opt. Soc. Am. A **13** (1996) 1870–1876.

[26] Y. J. Cao, Z. L. Hou, Y. Y. Liu: Convergence problem of plane-wave expansion method for phononic crystals. Phys. Lett. A **327** (2004) 247–253.

[27] J. H. Yuan, Y. Y. Lu, X. Antoine: Modeling photonic crystals by boundary integral equations and Dirichlet-to-Neumann maps. J. Comput. Phys. **227** (2008) 4617–4629.

[28] Y. X. Huang, Y. Y. Lu: Scattering from periodic arrays of cylinders by Dirichlet-to-Neumann maps. J. Lightwave. Tech. **4** (2006) 3448–3453.